

THE EFFECT OF THE SLED INSTALLATION ON EXTRACTED AND LOST BEAM AT THE AUSTRALIAN SYNCHROTRON LINAC

P. J. Giansiracusa*, T. G. Lucas, M. Volpi, R. P. Rassool,
The University of Melbourne, School of Physics, Melbourne, Australia
M. P. Lafky, The Australian Synchrotron ANSTO, Clayton, Australia
M. J. Boland, Canadian Light Source and Department of Physics and Engineering Physics,
University of Saskatchewan, Canada

Abstract

A recent upgrade to the high power RF network of the linac at the Australian Synchrotron (AS) included a SLED Type 1 Pulse Compressor which has allowed for the operation of the 100 MeV linac using a single klystron. We explore the effects of the SLED installation on the properties of the beam extracted from the linac with a particular focus on the energy spread and bunch train profile. Additionally, the optical fibre beam loss monitor (oBLM), also recently commissioned, was employed to provide shot-by-shot feedback on loss location and intensity to investigate the change in beam losses.

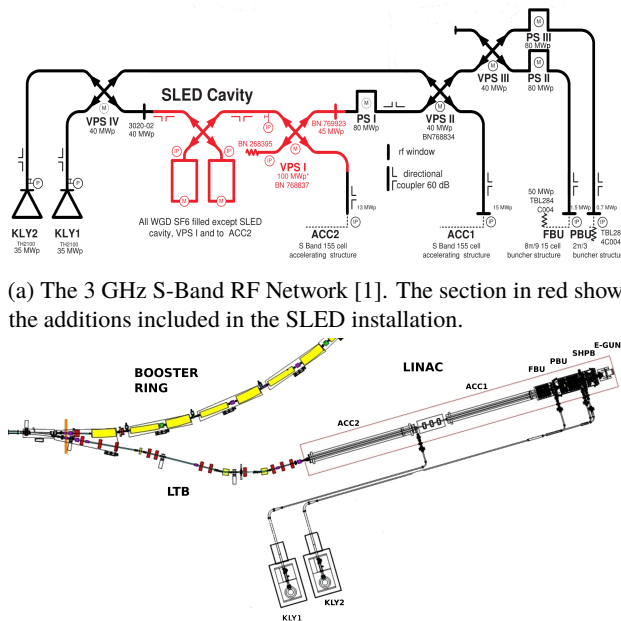
INTRODUCTION

A Stanford linac energy doubler (SLED) Type 1 Pulse Compressor (PC) was recently installed on the 3 GHz radio frequency (RF) power distribution network of the Australian Synchrotron (AS) [1]. The 3 GHz RF network powers the linac, the first stage of the AS injection system, which produces a 100 MeV electron beam. The beam is further accelerated by the booster synchrotron to 3 GeV for full energy injection into the storage ring. Prior to the installation of the SLED two klystrons were required to power the RF network. A failure of either klystron would prevent operation of the linac and block injection. With the installation of the SLED, the RF network can now be powered using a single klystron thereby mitigating the risk of single point failure.

The inclusion of the SLED changes the structure of the RF pulse delivered by the RF network to the accelerating structures, and consequently alters the beam produced. Here we investigate the effect on the beam by measuring the energy spread and bunch-train profile following extraction from the linac, with and without the use of the SLED. Additionally, the effect of the SLED on beam losses is explored with the use of the optical fibre beam loss monitor (oBLM), also recently commissioned, enabling shot-by-shot monitoring of loss location and intensity along the injection system.

THE 100 MEV INJECTION SYSTEM

Power for the 100 MeV injection system is produced by two pulsed 35 MW, 3 GHz klystrons (KLY1 and KLY2). The klystrons can be operated in tandem or using a single klystron in conjunction with the SLED. The RF power produced supplies the bunching structures, primary bunching



(a) The 3 GHz S-Band RF Network [1]. The section in red shows the additions included in the SLED installation.

(b) The layout of the 100 MeV injection system and transfer line.

Figure 1: A diagram of the RF network and the layout of the linac and LTB.

unit (PBU) and final bunching unit (FBU), and the accelerating structures, ACC1 and ACC2, of the linac. The power can be divided and directed to each of the structures with the aid of variable power splitters (VPS or hybrids) and phase shifters (PS). A diagram of the network is presented in Figure 1 (a). The power and phase of the RF input to each of the structures and at several locations within the network are monitored via directional couplers, the signals from which are down-converted to an intermediate frequency and digitised at 125 MS/s [2].

The power multiplication effect of the SLED is achieved by storing energy from the start of an RF pulse in both high Q cavities. A 180 ° phase shift is then applied to the pulse releasing the stored energy and adding it to the tail end of the pulse. In this way pulse length can be exchanged for peak power. A full description on the operation of the AS SLED can be found in [1].

Beam for the linac is supplied by a 90 kV thermionic electron gun and velocity modulated by a 500 MHz sub-harmonic pre-buncher (SHPB). A system of thirty one solenoids are employed to ease beam blowup in the low-

energy region of the linac and a quadrupole triplet provides focusing between the two accelerating structures [3–5]. The key parameters of the linac are summarised in Table 1. The beam exits the linac with a nominal energy of 100 MeV and is transferred to the booster synchrotron via the linac to booster (LTB) transfer line.

Table 1: Key Parameters of the AS Accelerating Structures and Linac

Parameter	Value
RF Frequency	2997 MHz
Acc. Struct. Fill Time	740 ns
Operating Temperature	40 °C
Nominal Energy	100 MeV
Repetition Rate	1-5 Hz
Normalised Emittance	50π mm.mrad
End Charge (single/multi)	>0.5 / >4.0 nC
Pulse Length (single/multi)	1 / 150 ns

Beam properties along the linac and LTB are monitored with the aid of several diagnostics. A wall current monitor (WCM) and two fast current transformers (FCTs) measure the bunch charge and longitudinal profile. YAG screens, monitored by cameras, can be inserted to intersect the beam and measure its dimensions. Beam losses along the length of the linac and LTB are also monitored with the optical fibre beam-loss monitor (oBLM) [6].

PROCEDURE

The structure of the RF pulse at the input to ACC1 with and without the SLED enabled is shown in Figure 2. A distinct difference between the two pulses is evident and provides the motivation for this work.

The use of the SLED is controlled via the tuning of the cavities in combination with an RF hybrid. When in use the SLED cavities are tuned by regulation of the temperature at 40° C and when not in use the temperature is lowered to 20° C, thereby moving the cavities sufficiently off resonance such that the RF pulse bypasses their inputs. Changing the

mode of operation between running with the SLED and without the SLED requires re-phasing of the RF network to successfully inject into the booster ring. This is the case independent of set points. As such, when a mode change is referred to in this report it refers to the enabling/disabling of the SLED and the required re-phasing.

Shot-by-shot data was collected for both modes of operation, with a nominal bunch charge of 400 pC for each. FCT measurements of the bunch train length showed that, with tuning, the nominal bunch train length of 150 ns could be achieved in both modes of operation.

Measurements of the beam energy spread were performed using the first dipole following the linac and a YAG screen, with a quadrupole between the two disabled. Background images were subtracted from the images collected and the field of view around the beam spots truncated to a region of interest. Averages of the resulting beams spots are shown in the upper plots of Figure 3. Summing along the vertical axis produced the two distributions, shown in the lower to plots of Figure 3, and a Gaussian curve was fitted to each. Both distributions show a sharp drop at pixel 630 as such data beyond this point was excluded from the fit. Using the location of the screen and the pixel size an estimate of the energy spread, neglecting emittance contributions, for each mode of operation could be made. The energy spread of the average beam spots calculated from the plots shown in Figure 3 were found to be 1.22 % and 1.20 % for the SLED enabled and disabled, respectively. While the mean energy spread within individual shots was found to be 1.09 % and 1.03 % with the SLED again enabled and disabled, respectively. Though the SLED produces a slightly higher result in both cases the uncertainty in the measurement is approximately ten percent and therefore no significant effect on the energy spread appears to be present. In both cases this result is slightly larger than previous measurements of the energy spread, ~0.7-0.8 % [4, 5], made earlier in the lifetime of the linac and before the installation of the SLED and will be further investigated in the future.

The oBLM detects beam losses via the Cherenkov mechanism using two optical fibres either side of the beam pipe. The loss signals with respect to location as recorded by the oBLM are shown in Figure 4. Signals from the fibre running on the outside of the curve of the LTB are shown as positive while those from the fibre on the inside of the curve are shown as negative. It is evident that there is a significant difference between the loss signals when operating with the SLED enabled and disabled, the solid blue and red lines, respectively. With much more beam lost when operating without the SLED, particularly towards the inside of the LTB. However, at the time that the measurements were carried out, the AS had been operating using the SLED for over a year and the injection efficiency into the booster had been increased significantly by tuning the linac solenoids and LTB lattice [7]. As such, the difference in the loss signals is attributed to the lattice having been tuned for operation with the SLED at the time of measurement. To verify this hypothesis a loss signal collected before significant tuning was also

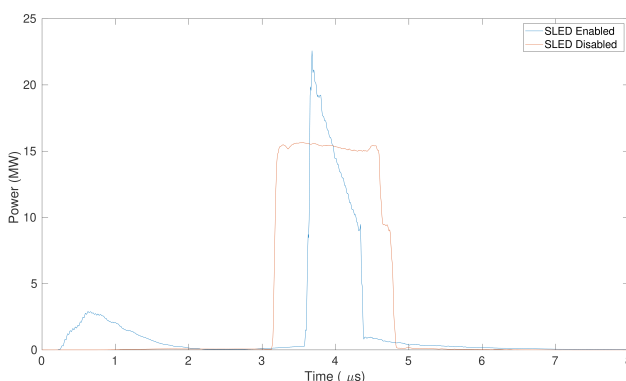


Figure 2: The difference in RF pulses input into the first accelerating structure with and without the SLED.

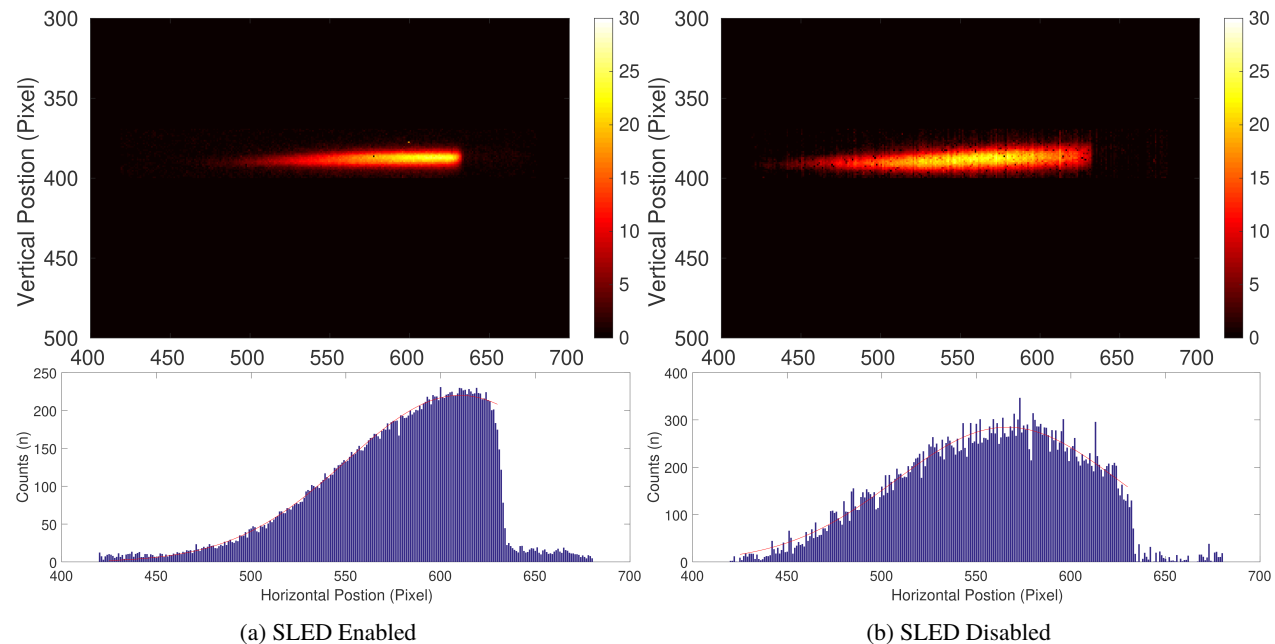


Figure 3: The upper plots show average beam spots recorded using the YAG screen with and without the SLED. The lower plots show the resulting horizontal distributions used to determine the relative energy spread.

plotted (dotted blue line). It shows that tuning has occurred, but also that there are likely differences attributable to the operation with the SLED as well.

CONCLUSION

The installation of the SLED changed the structure of the RF pulse provided to the linac. No significant differences in the beam energy spread or bunch train length were observed. Loss signals following the linac did show an increase when operating without the SLED. The differences observed appear to be in part due to the tuning of the linac and lattice. Future work will investigate this effect and in-particular

whether a similar result is observed when changing which klystron is used in combination with the SLED.

ACKNOWLEDGEMENTS

The authors would like to thank the operators, RF engineers and physics staff of the Australian Synchrotron for their help and willingness to change RF modes.

REFERENCES

- [1] K. Zingre, B. Mountford, M. P. Atkinson, R. T. Dowd, G. LeBlanc, and C. G. Hollwich, “Proposed Linac Upgrade with a SLED Cavity at the Australian Synchrotron, SLSA”, in *Proc. 6th Int. Particle Accelerator Conf. (IPAC’15)*, Richmond, VA, USA, May 2015, pp. 2738–2740. doi:10.18429/JACoW-IPAC2015-WEPMA001
- [2] P. Corlett, S. Chen, R. Hogan, G. LeBlanc, A. Michalczyk, A. Starratt, K. Zingre, “3GHz Linac RF measurement system using micro-TCA technology”, in *Post. 8th Low-Level RF Workshop (LLRF2017)*, Barcelona, Spain, Oct. 2017, poster P-18.
- [3] C. Christou, K. Dunkel, V. Kempson, and C. Piel, “The Pre-Injector Linac for the Diamond Light Source”, in *Proc. 22nd Linear Accelerator Conf. (LINAC’04)*, Lübeck, Germany, Aug. 2004, paper MOP21, pp. 84–86.
- [4] C. Piel *et al.*, “Commissioning of the Australian Synchrotron Injector RF Systems”, in *Proc. 10th European Particle Accelerator Conf. (EPAC’06)*, Edinburgh, UK, Jun. 2006, paper THPLS012, pp. 3293–3295.
- [5] R. T. Dowd, G. LeBlanc, and K. Zingre, “Linac Waveguide Upgrade at the Australian Synchrotron Light Source”, in *Proc. 2nd Int. Particle Accelerator Conf. (IPAC’11)*, San Sebastian, Spain, Sep. 2011, paper MOPC001, pp. 62–64.

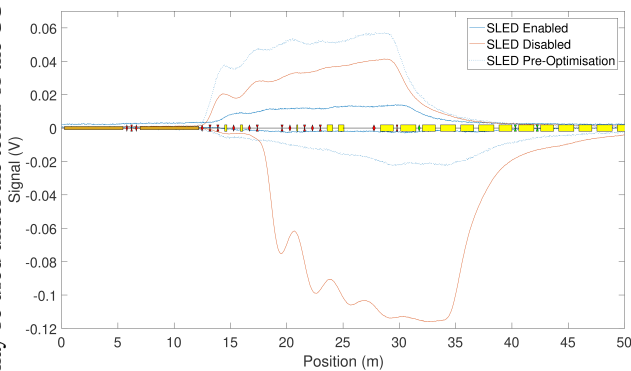


Figure 4: The loss signals along the linac and LTB collected using the oBLM. The solid and dotted blue curves show the loss signals when operating with the SLED before and after lattice optimisation, respectively. The red curves show the loss signals when operating without the SLED. A model of the linac and LTB is shown along the central axis.

- [6] P. J. Giansiracusa, and M. J. Boland, E. B. Holzer, M. Kas-triotou, G. S. LeBlanc, T. G. Lucas, E. Nebot del Busto, R. P. Rassool, M. Volpi, C. P. Welsch, “A distributed beam loss monitor for the Australian Synchrotron”, in *Nucl. Instr. Meth. Phys. Res. A*, 919, 98-104, 2019, Elsevier.
- [7] M. P. Lafky, “Improvements to Injector System Efficiency at the Australian Synchrotron”, presented at the 10th Int. Particle Accelerator Conf. (IPAC'19), Melbourne, Australia, May 2019, paper TUPGW001, this conference.